DOI: 10.1002/chem.200700383

Tetraazaperopyrenes: A New Class of Multifunctional Chromophores

Till Riehm,[a] Gabriele De Paoli,[b] Asgeir E. Konradsson,[b] Luisa De Cola,*[b] Hubert Wadepohl,[a] and Lutz H. Gade*[a]

Dedicated to Professor Mary McPartlin

Abstract: Tetraazaperopyrene and a range of derivatives have been synthesised and their photophysical and redox-chemical properties studied. The parent compound, 1,3,8,10-tetraazaperopyrene (**1**), was prepared by treating 4,9-diamino-3,10-perylenequinone diimine with triethyl orthoformate, whereas the 2,9-disubstituted derivatives of **1** were obtained after treatment with the corresponding carboxylic acid chloride or anhydride (2 mol equiv). The 1,3,8,10-tetraazaperopyrene core structure was established by X-ray diffraction of 2,9-bis(2-bromophenyl)-1,3,8,10-tetraazaperopyrene (**6**). The UV-visible absorption spectra of the compounds have a characteristic visible $\pi^*\leftarrow\pi$ absorption band at 440 nm ($\log\varepsilon_{max}=4.80$) with a strong vibrational progression ($\Delta\nu \approx 1450\ \text{cm}^{-1}$). Diprotonation of the nitrogen atoms induces a bathochromic shift of this band from 430–440 to 470–480 nm and all four nitrogen atoms are protonated when pure H_2SO_4 is used as the solvent. The first and second as well as the third and fourth protonations occur concomitantly, which implies that they have very similar pK_a values and, consequently, similar proton affinities. A theoretical study of the proton affinities in the gas phase and in solution attributes this behaviour to the effects of polar solvents, which dampen the charge of a protonated site at the other end of the molecule and thus effectively decouple the two opposite pyrimidine units in the polycondensed aromatic compound. The photophysical data were modelled in a time-dependent DFT study of **1**, **1**H_2^{2+} and **1**H_4^{4+} in both the gas phase and in a polar solvent. All the dyes show weak fluorescence in organic solvents, however, their protonated conjugate acids show dramatically increased fluorescence intensity. All of the dyes undergo two electrochemically reversible one-electron reductions with cyclovoltammetric half-wave potentials at $E_{red1}\approx -0.9$ V and $E_{red2}\approx -1.3$ V (vs. SCE), which are associated with characteristic spectral changes.

Keywords: azaaromatics • cyclic voltammetry • dyes/pigments • fluorescence • proton affinity

Introduction

The synthesis of new polycyclic aromatic hydrocarbons (PAHs)[1] has regained considerable interest in recent years owing to their manifold applications in organic electronics.[2] Since the pioneering work in this area,[3] both organic polymers and small-molecule (mainly PAH) organic solids have been employed as conducting or semiconducting materials in the development of electronic devices.[4] Whereas p-channel organic semiconductors have been extensively studied, it is only recently that efficient n-type semiconducting materials that employ PAHs have been developed. One strategy for the synthesis of the latter is based on the use of nitrogen-containing oligoacenes, such as diphenylanthrazolines and tetraazaanthracene derivatives.[5–7]

Apart from their potential use in the development of molecule-based n-semiconductors, polycyclic azaaromatics are among the most widely employed Lewis basic (ligating) building blocks for the assembly of well-defined functional supramolecular aggregates.[8] Simple azaaromatics, such as pyrazine, 4,4′-bipyridine or their expanded condensed analogues, such as diazapyrene or eilatine derivatives, may act as ditopic building blocks, redox- and photoactive ligands and as chemical sensors.[9] An important aim when using

---

[a] T. Riehm, Prof. Dr. H. Wadepohl, Prof. Dr. L. H. Gade
Anorganisch-Chemisches Institut, Universität Heidelberg
Im Neuenheimer Feld 270, 69120 Heidelberg (Germany)
Fax: (+49) 6221-545609
E-mail: lutz.gade@uni-hd.de

[b] G. De Paoli, A. E. Konradsson, Prof. Dr. L. De Cola
Physikalisches Institut der Universität Münster
Mendelstraße 7, 48149 Münster (Germany)
Fax: (+49) 251-980-2834
E-mail: decola@uni-muenster.de

Supporting information for this article is available on the WWW under http://www.chemeurj.org/ or from the authors.

such dye molecules as functional structural units is the exploitation of their potentially rich photo and redox chemistry in ever more highly condensed systems.[10]

The work reported herein focussed on a new member of the azaperopyrene family that has rich photo and redox chemistry. Peropyrene (**A**) was first synthesised in 1943 by Clar who reductively coupled two molecules of perinaphthindenone with zinc and proposed the generic name for this compound.[11] Its electronic structure and photophysics have been studied in detail in recent years[12] and it is a highly efficient fluorophore with a quantum yield that approaches unity when dissolved in benzene.

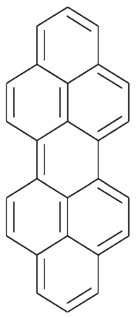
A

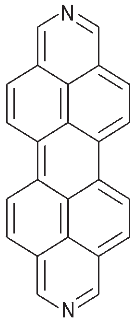
B

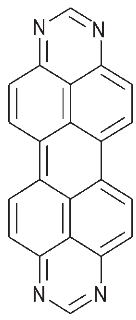
C

In contrast to this condensed heptacyclic aromatic hydrocarbon, diazaperopyrene (**B**) has been known for much longer. First reported in a German patent in 1913, diazaperopyrene derivatives have found applications as functional dyes.[13] The di-N-methylated dicationic derivative was found to interact strongly with nucleotide bases in single-stranded nucleic acids and to effect their photocleavage.[14] Notably, it also has nucleotide base-dependent emission behaviour. Stang et al. reported the use of diazaperopyrene as a difunctional molecular spacer in the construction of polynuclear molecular squares by connecting square planar Pd^{II} or Pt^{II} complex fragments.[15] In these applications, the low solubility of the dye molecules limited the practicability of their use as molecular building blocks.[16]

Tetraaza analogue **C** has not been reported to date, however, early reports by Zinke et al. on the functionalisation of 4,9-diamino-3,10-perylenequinone diimine (DPDI) indicate that they isolated a dimethylated derivative that was erroneously formulated as the corresponding dihydrogenated compound.[17]

Recently, we developed an efficient metal-induced synthesis of DPDI by oxidative coupling of two 1,8-diaminonaphthalene molecules.[18] The availability of this starting material allowed us to synthesise, for the first time, tetraazaperopyrene as well as a range of derivatives and to study their photophysical and redox-chemical properties.

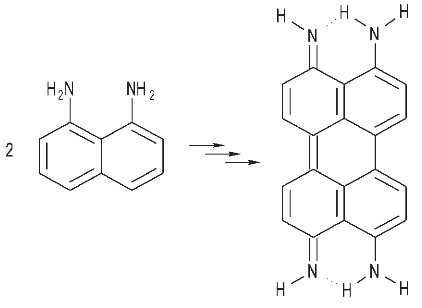
DPDI

Results and Discussion

Synthesis of 1,3,8,10-tetraazaperopyrene and its derivatives: The parent compound, 1,3,8,10-tetraazaperopyrene (**1**), was prepared by treating DPDI with triethyl orthoformate in the presence of catalytic amounts of formic acid and purified by sublimation in high vacuum. The elemental analysis is consistent with its formulation as $C_{22}H_{10}N_4$. The yellow-brown compound is only sparingly soluble in organic solvents, but readily dissolves in H_2SO_4. Solutions of the N-deuterated tetracation (see below) were characterised by ^1H and ^{13}C NMR spectroscopy. 2,9-Disubstituted derivatives of **1** are readily accessible by treating DPDI either with the corresponding carboxylic acid chloride or anhydride (2 mol equiv) in the presence of triethylamine in THF or with a large excess of acid chloride or anhydride in nitrobenzene at reflux (Scheme 1).

Whereas the study of the properties of the 2,9-dimethylated derivative **2** in solution is limited by its low solubility, the *tert*-butyl- and 1-adamantyl-substituted derivatives **3** and **4**, respectively, are soluble in polar organic solvents. Compounds with long-chain alkyl groups, such as **5a** and **5b**, are soluble in virtually all polar organic solvents; thus, there is the potential for a comprehensive study of their redox chemistry and photophysics.

Among the 2,9-diarylated derivatives only the *ortho*-substituted phenyl derivatives, compounds **6** and **7**, had sufficient solubility for further characterisation in solution. This may be due to the twist of the aryl substituent, which is imposed by the steric repulsion between the *ortho* substituents and the peropyrene core and impedes efficient aromatic stacking upon crystallisation (see below). This observation is not unlike the situation observed by Würthner and Seybold for their bay-substituted diazaperopyrene derivatives, which also have good solubility as a result of perturbed molecular stacking.[19] Compound **7** may be obtained either directly by treating DPDI with phthalic anhydride (2 mol equiv) or by lithiation of **6** with *n*BuLi and subsequent reaction with CO_2.

With the exception of **7**, all of the new compounds display remarkable thermal stability up to 400 °C. Their decomposition points were studied by differential thermal analysis (DTA) and thermogravimetric analysis (TGA) and were found to be above that temperature (see the Experimental

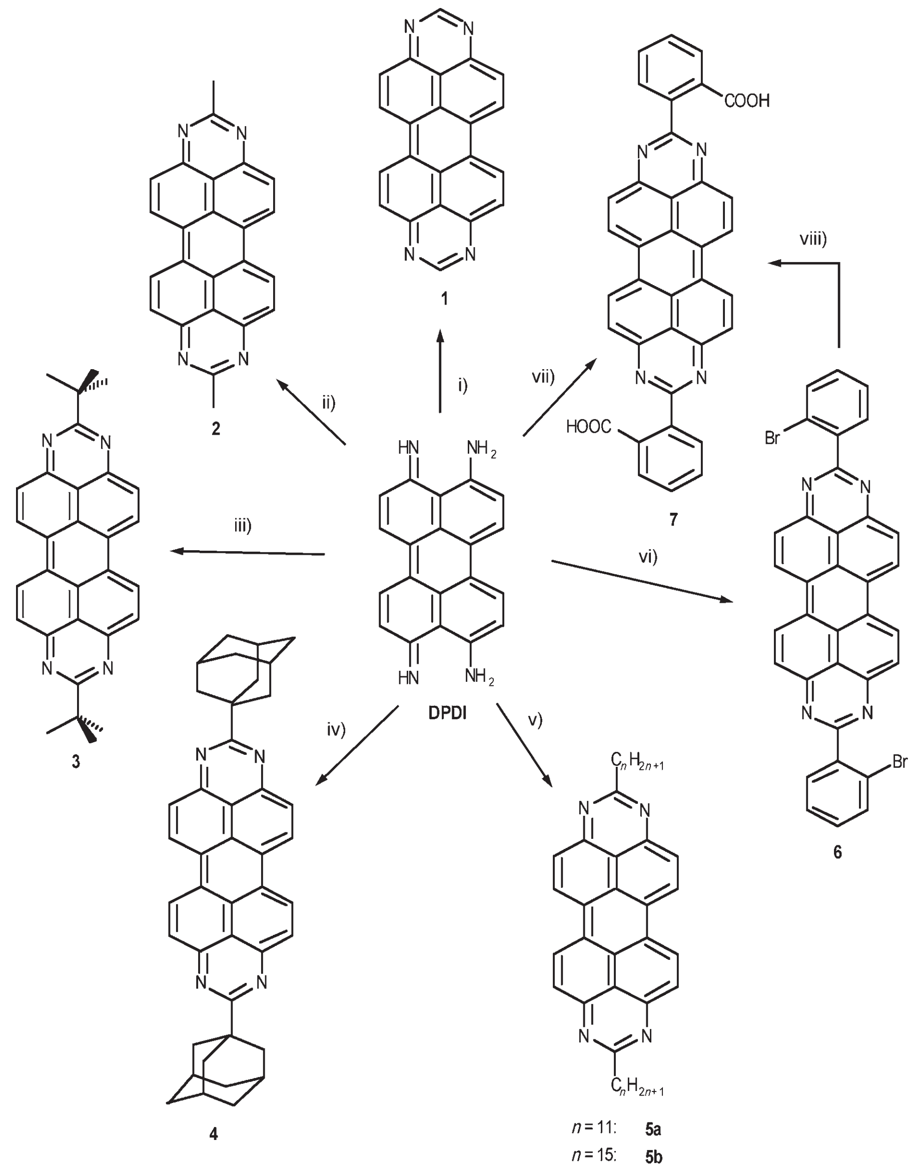

Scheme 1. Synthesis of tetraazaperopyrene (**1**) and its derivatives **2**–**7**. Reagents and conditions: i) triethyl orthoformate, cat. formic acid, reflux; ii) acetic anhydride, nitrobenzene, reflux; iii) trimethylacetyl chloride, triethylamine, THF, reflux; iv) adamantanecarboxylic acid chloride, nitrobenzene, reflux; v) $C_nH_{2n+1}COCl$, triethylamine, THF, reflux; vi) *o*-bromobenzoyl chloride, nitrobenzene, reflux; vii) phthalic anhydride, nitrobenzene, reflux; viii) *n*BuLi, CO_2, THF, −30 °C.

Section). The dyes are stable in air and do not decompose upon dissolution in concentrated sulfuric acid.

Crystal structure of 2,9-bis(2-bromophenyl)-1,3,8,10-tetraazaperopyrene (6): Crystals of compound **6** suitable for X-ray diffraction were grown from nitrobenzene. The molecular structure is shown in Figure 1 along with selected bond lengths and angles.

The molecule has a crystallographic centre of symmetry that relates its two opposite halves. Not unexpectedly, the bond length patterns in **6** closely resemble those previously observed in DPDI derivatives[18] rather than the metric data obtained by Würthner and co-workers for the diazaperopyrenes,[16a,d] which are formally and chemically more closely related to the intensively studied perylenetetracarboxdiimides.[20] For example, the mean bond lengths in the perylene core of compound **6**, C(11)−C(10) and C(5)−C(6) (1.353 Å) and C(7)−C(9a) (1.410 Å), are very similar to the corresponding bond lengths in the silylated DPDI derivatives (1.341 and 1.421 Å, respectively).[18a,b] On the other hand, these bond lengths are significantly shorter than the analogous values in perylene (1.40 and 1.48 Å) and its derivatives.[20] The tetraazaperopyrene core is virtually planar, whereas the two 2-bromophenyl rings are tilted (dihedral angle 52°) as a consequence of the steric repulsion between the bromo substituents and the nitrogen atoms of the polycondensed aromatic core.

The crystal structures of a large number of perylene bisimides have been studied to investigate the correlation between molecular packing and colour in pigments.[21] In most derivatives that possess a planar structure and no bulky substituents, parallel stacking of the molecules occurs with an interplane distance of between 3.34 and 3.55 Å (the distance in graphite is 3.35 Å). Parallel stacking is also present in the crystal structure of **6** (Figure 2); the distance of 4.00 Å between the herringbone layers of **6** is a rare example of a π–π stacking distance significantly greater than the norm. In the case at hand, the tilted bulky 2-bromophenyl substituent prevents tighter packing and the bromine atoms are weakly hydrogen-bonded to hydrogen atoms in the *para* position of the neighbouring phenyl groups (Br−HC = 2.82 Å).

UV-visible absorption spectra of the 2,9-dialkyl-1,3,8,10-tetraazaperopyrenes (2–5) and their di- and tetraprotonated conjugate acids: All of the tetraazaperopyrene derivatives (**2**–**5**) are orange to yellow-brown in the solid state and yellow to orange in solution, depending on the concentration. The UV-visible absorption spectra of **2**–**5** recorded in toluene are almost superimposable and display a characteristic visible absorption band between 380 and 440 nm ($\log \varepsilon_{max} = 4.80$, Table 1). The band is characterised by a strong vibrational progression ($\Delta\nu \approx 1450\, cm^{-1}$) as is typical for $\pi^{*} \leftarrow \pi$ transitions in polycondensed aromatics and in particular for perylene derivatives.[22] The UV-visible absorption spectra of compounds **5a** and **5b** are shown in Figure 3.

Table 1. $\pi^{*} \leftarrow \pi$ Transitions [nm] in the absorption spectra recorded in different solvents.

Compound	Toluene		CF_3COOH		H_2SO_4	
	$\lambda_{max1}(\log \varepsilon_1)$	$\lambda_{max2}(\log \varepsilon_2)$	$\lambda_{max1}(\log \varepsilon_1)$	$\lambda_{max2}(\log \varepsilon_2)$	$\lambda_{max1}(\log \varepsilon_1)$	$\lambda_{max2}(\log \varepsilon_2)$
1	434	408[a]	471	441[a]	506 (4.79)	473 (4.37)
2	437	409[a]	473 (4.56)	444 (4.36)	505 (4.87)	472 (4.42)
3	432 (4.86)	409 (4.64)	474 (4.63)	445 (4.40)	509 (5.08)	475 (4.55)
4	436 (4.64)	410 (4.44)	472 (4.94)	443 (4.69)	512 (5.06)	478 (4.62)
5a	437 (4.80)	411 (4.61)	476 (4.82)	447 (4.60)	507 (5.09)	473 (4.68)
5b	437 (4.52)	411 (4.61)	475 (4.74)	446 (4.48)	507	473[a]
6	440 (4.16)	414 (3.95)	481 (4.88)	451 (4.63)	512 (4.93)	478 (4.53)
7	–	–	478 (4.89)	450 (4.63)	510 (4.95)	477 (4.57)

[a] Owing to the low solubility of the compound in the respective solvent the (saturated) solutions were of undefined concentration and the molar extinction coefficients were not determined.

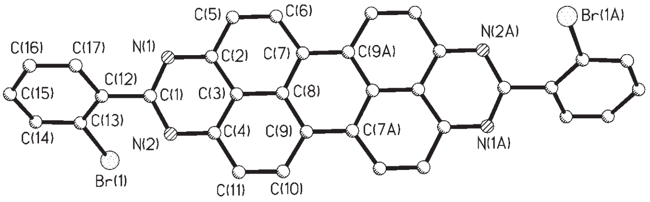

Figure 1. Molecular structure of compound **6**. Principal bond lengths [Å] and angles [°]: Br(1)–C(13) 1.926(3), C(1)–N(1) 1.313(3), C(1)–N(2) 1.336(3), C(1)–C(12) 1.478(3), C(2)–N(1) 1.339(3), C(2)–C(5) 1.394(3), C(2)–C(3) 1.403(3), C(3)–C(4) 1.376(3), C(3)–C(8) 1.413(3), C(4)–N(2) 1.342(3), C(4)–C(11) 1.422(4), C(5)–C(6) 1.350(4), C(6)–C(7) 1.430(3), C(7)–C(8) 1.393(3), C(7)–C(9) 1.410(3), C(8)–C(9) 1.413(3), C(9)–C(10) 1.410(3), C(9)–C(7) 1.410(3), C(10)–C(11) 1.356(4), C(12)–C(13) 1.408(4), C(12)–C(17) 1.450(4), C(13)–C(14) 1.379(4), C(14)–C(15) 1.407(4), C(15)–C(16) 1.396(4), C(16)–C(17) 1.357(4); N(1)-C(1)-N(2) 126.9(2), N(1)-C(1)-C(12) 114.5(2), N(2)-C(1)-C(12) 118.6(2), N(1)-C(2)-C(5) 118.7(2), N(1)-C(2)-C(3) 122.8(2), N(2)-C(4)-C(3) 120.8(2), N(2)-C(4)-C(11) 120.8(2), C(14)-C(13)-Br(1) 115.7(2), C(12)-C(13)-Br(1) 123.24(19), C(1)-N(1)-C(2) 115.4(2), C(1)-N(2)-C(4) 117.4(2).

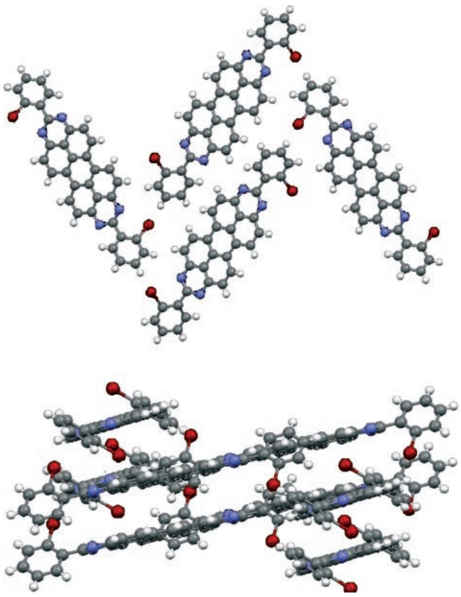

Figure 2. Top: Packing of the molecules of **6** in the crystal form showing the weak intermolecular C–Br···H–C hydrogen bonds. Bottom: Crystal packing of **6** showing the twisted arrangement of the *o*-bromophenyl substituents relative to the tetraazaperopyrene core.

Notably, we found that the tetraazaperopyrenes are only relatively weak bases and, thus, require strongly acidic conditions to render their protonated conjugate acids. The titration of **5b** with CH_3SO_3H in toluene was monitored by UV-visible spectroscopy and the spectra recorded after the addition of one and two molar equivalents of acid are shown in Figure 4. Upon addition of one equivalent of the acid, two superimposed bands of the $\pi^{*} \leftarrow \pi$ transitions of **5b** and its diprotonated derivative **5b**H_2^{2+} were observed, the conversion was complete after the addition of the second equivalent of methanesulfonic acid. The observation of well-defined isosbestic points supports the notion of a clean and selective conversion of **5b** to **5b**H_2^{2+}.

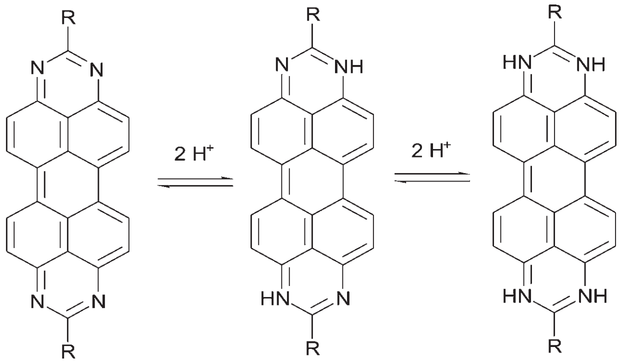

The diprotonation is shown by a bathochromic shift of the maximum of the $\pi^{*} \leftarrow \pi$ band from 430–440 to 470–480 nm (Figure 4) and may also be monitored by the downfield shift of the AB proton resonance system of the central perylenic core from $\delta = 8.79$ to 10.35 ppm. The fact that the monoprotonated species was not observed is attributed to the distance between the two protonation sites, which renders the two pK_a values almost identical. Whereas the addition of trifluoroacetic acid ($pK_a = 0.23$ in H_2O) did not lead to the formation of **5b**H_2^{2+}, the use of methanesulfonic acid ($pK_a = -1.9$ in H_2O) cleanly gave the diprotonated species. Therefore, the acidity of **5b**H^{+} and **5b**H_2^{2+} corresponds to pK_a values lying between around 0 and −1 in aqueous media (in which the peropyrenes are insoluble).

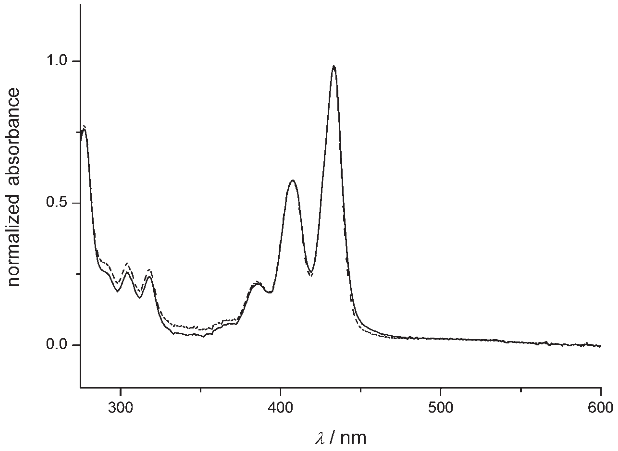

Figure 3. Normalised absorption spectra of aerated solutions of **5a** and **5b** in THF.

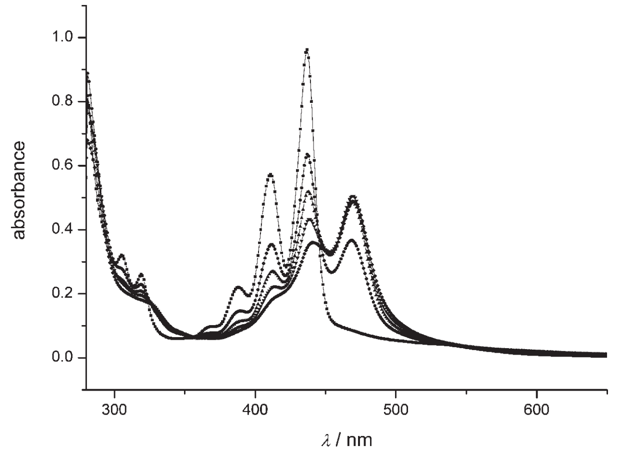

Figure 4. Titration of compound **5b** in toluene with methanesulfonic acid to generate the diprotonated dicationic species **5b**H_2^{2+}, the π*←π band displaying the characteristic bathochromic shift. ■: 0 equiv, ●: 0.5 equiv, ▲: 1 equiv, ▼: 1.5 equiv, ◆: 2 equiv.

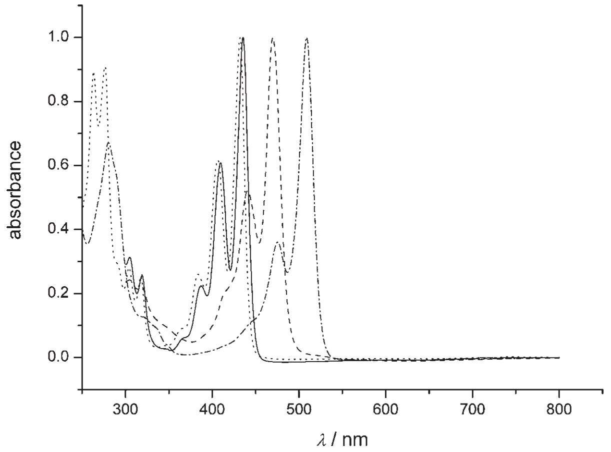

Figure 5. Normalised UV-visible absorption spectra of compound **3** dissolved in different solvents (—— toluene, ••••• THF, ----- TFA and –•–• sulfuric acid). Notice that the main species is **3** in toluene and THF, **3**H_2^{2+} in TFA and **3**H_4^{4+} in sulfuric acid.

Upon going to an even more acidic medium, all four nitrogen atoms in the tetraazaperopyrene could be protonated to give tetracationic molecular dyes.

The UV-visible absorption spectra of *tert*-butyl-substituted derivative **3**, which were recorded in toluene, THF, trifluoroacetic acid (TFA) and in neat H_2SO_4, are depicted in Figure 5. Although the $\pi^*\leftarrow\pi$ band recorded in neat CF_3COOH displays the 40 nm bathochromic shift established for the diprotonated dye (and thus illustrates the greater protonating capability of the pure acid compared with its solutions in toluene, see above), a further shift of 45 nm to higher wavelengths is observed in the spectrum recorded in pure H_2SO_4 (Table 1).

Theoretical modelling of the acid–base behaviour of tetraazaperopyrene: Calculating the pK_a values of acids and bases both in water and in non-aqueous solvents has proven to be a difficult challenge in the theoretical modelling of the properties of molecular compounds.[23] This is challenging primarily owing to the sensitivity of the acid/base constants to the thermodynamic functions and consequently the large errors that result from approximate solutions. Liptak, Shields and co-workers recently devised a successful strategy for calculating the pK_a values of several classes of molecules, optimising their structures with large basis sets at the MP2 level of theory and taking the solvent environment into account by way of the conductor polarisable continuum model (CPCM).[24] This strategy gives excellent agreement with experimental data for small molecules such as pyrimidine, which is a structural motif present in the tertraazaperopyrenes. However, the required level of computational accuracy cannot be attained by the same means for molecules of the size discussed in this paper. Also, a reliable estimate of the heat of solvation of the proton in media relevant to this work was not possible. Therefore, we focussed on the proton affinities (PAs) of the different protonated derivatives of **1**, which correlate with the pK_a values and, in particular for solution-phase models, provide a rapid method for determining relative basicities.[25–27]

The gas-phase PA of a molecule (M) is defined as $PA = H(M) + H(H^+) - H(MH^+)$ in which the molar enthalpy of the proton $H(H^+)$ is generally fixed at $2.5RT = 1.48$ kcal mol^{-1}; the related gas-phase basicity (GB) is given by $GB = G(M) + G(H^+) - G(MH^+)$.[26] For the free enthalpy of the proton, the value of $G(H^+) = -6.28$ kcal mol^{-1} has previously been derived.[27]

The ground-state geometries of **1** and its mono-, di-, tri- and tetraprotonated derivatives, **1**H^+, **1**H_2^{2+}, **1**H_3^{3+} and **1**H_4^{4+}, were optimised by DFT methods by using the B3PW91 functional and a 6-31g(d,p) basis set followed by a frequency calculation to verify the energy minima. In general, good agreement with the metric parameters of the tetraazaperopyrene core in crystallographically characterised derivative **6** was obtained, the deviations are attributable to the non-symmetrical aryl substituent in the latter. The gas-phase PAs were calculated by using the thermodynamic data obtained from these frequency calculations. The calculated data for **1**, **1**H^{+}, **1**H$_2^{2+}$ and **1**H$_3^{3+}$ are summarised in Table 2.

Table 2. Gas-phase PAs and basicities for protonated forms of **1**.

Compound	PA[a] [kJ mol^{-1}]	Gas-phase basicity [kJ mol^{-1}]
1	993.76	962.39
1H^{+}	736.84	704.95
1H$_2^{2+}$	381.19	349.19
1H$_3^{3+}$	126.55	92.46

[a] Calculated by using the DFT functional RB3PW91 and the 6-31G-(d,p) basis set.

We note that the sequential gas-phase PAs decrease as expected with increasing the degree of protonation of **1**, however, the energy increments between them are considerable and are apparently in contradiction to the experimental observation that the first and second as well as the third and fourth protonations occur concomitantly at the same acidity of the medium and, therefore, are expected to have very similar pK_a values and, consequently, similar PAs. The observed chemical behaviour must therefore be due to the effects of the polar solvents, which dampen the charge of a protonated site at the other end of the molecule and, thus, effectively decouple the two opposite pyrimidine units in the polycondensed aromatic compound. This interpretation was confirmed by calculating the PAs in a polar environment.

To this end, frequency calculations on the B3PW91/6-31g-(d,p)-optimised structure were performed with the B3LYP functional and a 3-21g basis set by using the CPCM model and water as the polar medium of reference. The solution PAs of **1**, **1**H^{+}, **1**H$_2^{2+}$ and **1**H$_3^{3+}$, along with those of pyrimidine and pyrimidineH^{+}, are summarised in Table 3.

Table 3. Calculated PAs in solution.[a]

Species	PA [kJ mol^{-1}]
1	1189
1H^{+}	1173
1H$_2^{2+}$	1117
1H$_3^{3+}$	1100
pyrimidine	1177
pyrimidineH^{+}	1097

[a] Geometry optimisation with B3PW91/6-31g(d,p), frequency calculation with B3LYP/3-21g.

The closely spaced PAs of **1** and **1**H^{+} (1189 and 1173 kJ mol^{-1}) are similar to that of pyrimidine in water (1177 kJ mol^{-1}), whereas the PAs of **1**H$_2^{2+}$ and **1**H$_3^{3+}$ are significantly offset (1117 and 1100 kJ mol^{-1}) and are similar in magnitude to that of pyrimidineH^{+} (1100 kJ mol^{-1}). It is thought that even an inversion of the first and second PAs may occur as a result of the influence of the counterions, although this feature cannot be modelled with the methods employed in this study. These results are consistent with the interpretation of the experimentally observed protonation behaviour given above.

Theoretical modelling of the absorption spectrum of tetraazaperopyrene and the changes associated with the protonation steps: A remarkable spectral feature of the tetraazaperopyrenes studied in this work is the bathochromic shift of the principal visible π*←π band at around 440 nm upon going from the neutral dyes to their di- and tetraprotonated conjugate acids. To study this characteristic in more detail, it has been modelled on the basis of the DFT structural calculations presented in the previous section.

The Kohn–Sham HOMOs and LUMOs of parent compound **1** as well as **1**H$_2^{2+}$ and **1**H$_4^{4+}$ are depicted in Figure 6. Both are π orbitals of the condensed aromatic ring system. Protonation of the nitrogen atoms leads, as expected, to a distortion of these frontier orbitals in the less symmetric derivative **1**H$_2^{2+}$, although the original symmetry is regained in the tetraprotonated species **1**H$_4^{4+}$. The overall nodal structures and the energetic spacing of the frontier orbital region remain essentially unchanged.

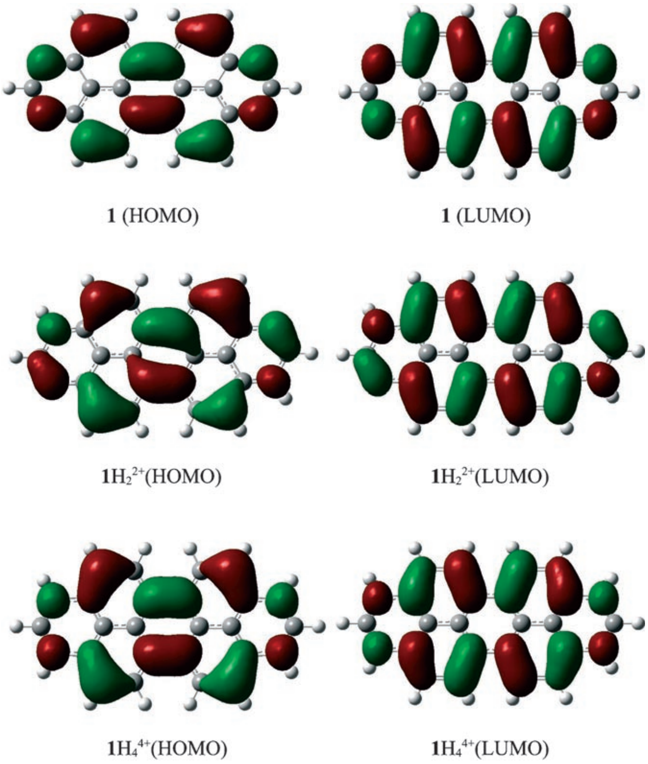

1 (HOMO) **1** (LUMO)

1H$_2^{2+}$(HOMO) **1**H$_2^{2+}$(LUMO)

1H$_4^{4+}$(HOMO) **1**H$_4^{4+}$(LUMO)

Figure 6. Kohn–Sham HOMOs (left) and LUMOs (right) of compound **1** and its di- and tetraprotonated forms **1**H$_2^{2+}$ (shown for one of the two possible isomers) and **1**H$_4^{4+}$, respectively.

The calculated gas-phase HOMO and LUMO energies for **1** and its conjugate acids are summarised in Table 4. Notable is the marked decrease in the HOMO–LUMO gap upon going from **1** to **1**H$_2^{2+}$ and then further to **1**H$_4^{4+}$, which correlates with the observed spectral behaviour. The experimental data was semi-quantitatively modelled by a time-dependent DFT (TDDFT) study of **1**, **1**H_2^{2+} and **1**H_4^{4+} carried out both in the gas phase and in a polar solvent medium. Although this theoretical method displays incorrect asymptotic behaviour in the modelling of excited states, it has generally been proven to give fairly reliable results for the transitions in molecules that are well below the ionisation level.[28,29]

Table 6. Photophysical properties[a] of the tetraazaperopyrenes.

	Toluene			CF$_3$COOH			H$_2$SO$_4$		
	Φ[b]	λ_{exc} [nm]	τ [ns]	Φ[c]	λ_{exc} [nm]	τ [ns]	Φ[c]	λ_{exc} [nm]	τ [ns]
1	0.01	402	1.1	0.47	431	17.7	0.34	431	3.4
2	0.02	402	1.0	0.41	431	17.2	0.43	431	3.9
3	0.01	431	1.0	0.53	431	18.6	0.48	431	2.8
4	0.01	431	1.5	0.22	431	8.3(54) 17.8(46)	0.01	431	1.8(30) 3.2(65)
5a	0.02	402	2.9	0.30	431	2.8	0.05	431	1.8(26) 5.2(65)
5b	0.01	402	1.5	0.34	431	1.6	0.04	431	
6	–	–	–	<0.001	431	4.2(52)	–	–	–
7	–	–	–	0.19	431	5.1	–	–	–

[a] Φ = emission quantum yields, λ_{exc} = excitation wavelengths used for measuring the excited-state lifetimes τ. The relative weights of the exponential curves are reported in parentheses. [b] A degassed solution of perylene in ethanol was used as the standard reference (see ref. [30]). [c] An aqueous solution (0.1 M in NaOH) of fluorescein was used as the standard reference (see ref. [31]).

Table 4. Kohn–Sham HOMO–LUMO gaps for compound **1** and its protonated forms.

	E(HOMO) [hartree]	E(LUMO) [hartree]	$E_{HOMO}-E_{LUMO}$ [nm]
1	−0.227	−0.118	418
1H^+	−0.351	−0.251	455
1H_2^{2+}	−0.476	−0.374	447
1H_3^{3+}	−0.599	−0.501	465
1H_4^{4+}	−0.723	−0.625	465

The results of this study, which are summarised in Table 5, clearly demonstrate that the influence of the solvent media has to be taken into account to model the observed spectral behaviour. The agreement with the experimental data is as good as can be expected for a TDDFT study at this level. The π*←π transition, which is dominated by the HOMO–LUMO excitation, is shifted from 443 nm in toluene to 483 nm in sulfuric acid (**1**H_4^{4+}), which indeed emulates the behaviour of all of the tetraazaperopyrene derivatives reported in this work.

Table 5. Position of the major visible π*←π transition of compound **1** calculated by time-dependent DFT for environments of different polarity.[a]

	λ (gas) [nm]	λ (solution) [nm]
1	422	443 (toluene)
1H_2^{2+}	458	467 (TFA)
1H_4^{4+}	468	483 (sulfuric acid)

[a] The HOMO–LUMO transition provides the major contribution to this transition.

Emission behaviour of the tetraazaperopyrenes: Compounds **2**–**5** display weak fluorescence in solutions of organic solvents (toluene, THF). The vibrationally structured emission mirrors the π*←π absorption band, which has its maximum at 445 nm and a Stokes shift of only 10 nm. The quantum yield for the emission is about 0.01 and the lifetime of the excited state was found to be between 1 and 3 ns (Table 6).

In contrast, the fluorescence intensity is dramatically increased upon going from the neutral dyes to their protonated conjugate acids (with excited-state lifetimes of up to 18 ns). For the diprotonated forms of the dyes, which are formed in neat CF$_3$COOH and display a bathochromically shifted fluorescence (λ_{max} = 477–490 nm), emission quantum yields of up to 53 % (**3**H_2^{2+}) were found (Table 6). The fluorescence band of the tetraazaperopyrene dye was further shifted to higher wavelengths (λ_{max} = 519–525 nm) upon going to the tetraprotonated derivative generated in neat H$_2$SO$_4$. Emission quantum yields of up to 48 % (**3**H_4^{4+}) were determined in this medium. Overall, the frequencies of the emission bands follow the protonation shift of the corresponding absorption band. The fluorescence spectra of **3**, **3**H_2^{2+} and **3**H_4^{4+} are depicted in Figure 7.

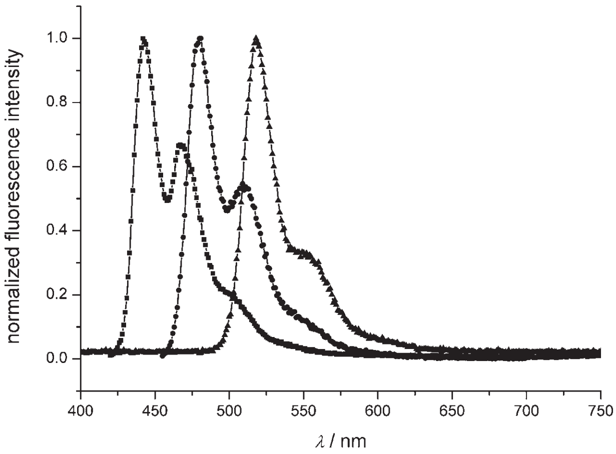

Figure 7. Normalised emission spectra of compound **1** dissolved in different media, toluene and THF (■, 408 nm), TFA (●, 450 nm), sulfuric acid (▲, 481 nm). The excitation wavelengths are given in parentheses.

For some of the protonated species, the fluorescence decay curves were found to be biexponential. This behaviour and the general photophysical properties of the dyes reported in this work were found to be concentration independent over a range of 10^{-5} to 10^{-6} M.

For some of the tetraazaperopyrene derivatives, notably compounds **2**, **4**, **5a** and **5b**, a reversible photoreaction in H_2SO_4 was observed, the nature of which remains to be established.

Electrochemistry of the 2,9-dialkyl-1,3,8,10-tetraazaperopyrenes (3–5) and a spectroelectrochemical study of 2,9-bis(undecyl)-1,3,8,10-tetraazaperopyrene (5a): The cyclic voltammograms of the soluble 2,9-dialkyl derivatives **3**–**5** display two reversible one-electron reduction waves that correspond to the sequential formation of the mono- and dianionic species. The electrochemical data are summarised in Table 7.

Table 7. Cyclovoltammetric data for compounds **2**–**5**.

Compound	E_1 [V][a]	E_2 [V]
2	−1.13	−1.47
3	−1.04	−1.41
4	−1.09	−1.43
5a	−1.11	−1.50
5b	−1.18	−1.49

[a] Potentials vs. SCE; spectra were recorded in THF.

The cyclic voltammogram of **5a** recorded at a sweep rate of $100\,mV\,s^{-1}$ in THF (Figure 8) displays two reversible redox waves with half-wave potentials at $E_{red1} = -0.87$ V and $E_{red2} = -1.26$ V (vs. SCE) with a difference between the cathodic and anodic wave of 88 mV in each case. The observation of an i_a/i_c ratio of exactly one and a relationship of $i_p \approx v^{1/2}$ indicates the reversibility of the electrochemical process, whereas recording the CV waves in the presence of ferrocene as an internal standard established them to be two one-electron reductions. The difference in the potentials of the two one-electron steps of 390 mV corresponds to a conproportionation constant of $K_c = 3\times10^6$.[32]

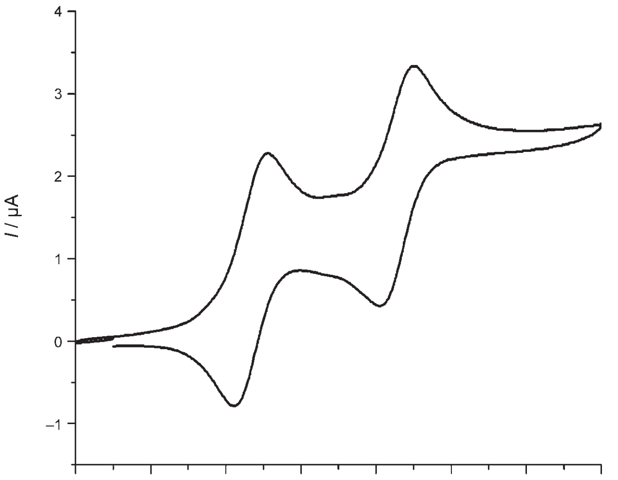

Figure 8. Cyclic voltammogram of **5a** recorded in THF (sweep rate: $100\,mV\,s^{-1}$; supporting electrolyte: NBu_4BF_4).

The first reduction step was monitored by UV-visible absorption spectroscopy in a spectroelectrochemical cell. Electrolysing the solution at a reduction potential of between −0.9 and −1.2 V revealed the formation of a deep-blue one-electron-reduced species. The absorption spectra of compound **5a** recorded during the course of the reduction are displayed in Figure 9.

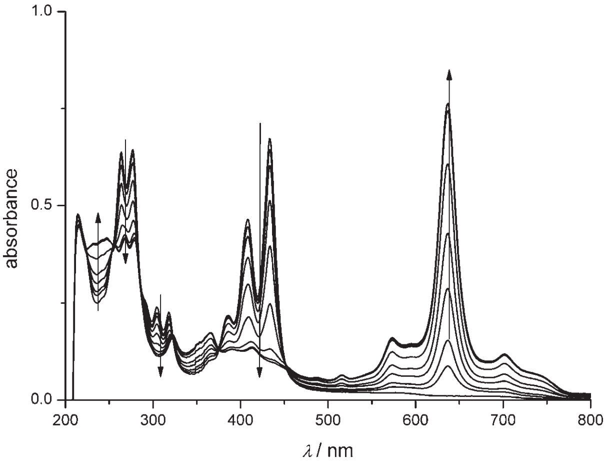

Figure 9. Spectroelectrochemical series for the first reduction step of compound **5a** to give the monoanion **5a**⁻. Cathodic potential: −0.9 to −1.2 V; recorded in THF.

The spectra, with their sharp isosbestic points, indicate that a clean electrochemical reduction of **5a** occurred. The most characteristic change in the absorption spectra is the disappearance of the vibrationally structured $\pi^* \leftarrow \pi$ band at 390–435 nm and the growing in of a very intense, highly structured, long-wavelength band with a maximum at 640 nm, which accounts for the blue colour of the one-electron-reduced tetraazaperopyrene dye.

A similar spectroelectrochemical sequence monitoring the conversion of the mono- to the dianionic reduction product was recorded during the course of the electrolysis of **5a** at −1.3 V and is depicted in Figure 10.

The change in the absorption spectra upon going from the mono- to the dianion is less pronounced than for the first one-electron reduction. Both species give blue solutions and the second reduction step is visually barely recognisable. The spectral changes in the region below 550 nm are relatively minor, whereas the sharp isosbestic points are consistent with the type of redox conversion proposed for this transformation. The most characteristic change in the spectral sequence in Figure 10 is the decrease in intensity of the absorption at 640 nm and the change from the sharply contoured band in this position of the monoanion to a broader absorption band between 550 and 700 nm. A comparative display of the UV-visible absorption spectra of the neutral tetraazaperopyrene **5a** as well as its mono- and dianion is shown in Figure 11.

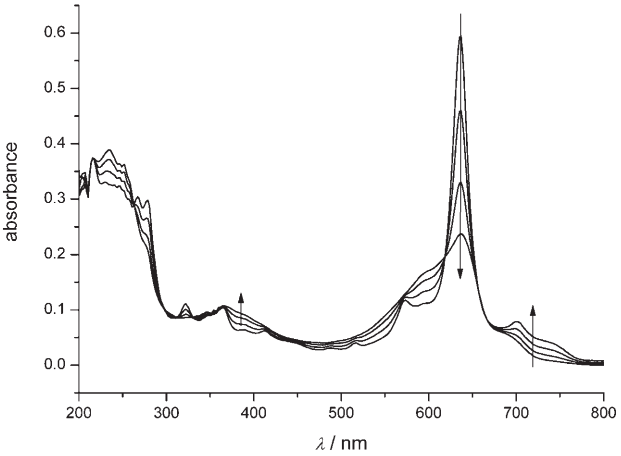

Figure 10. Spectroelectrochemical series for the second reduction step of compound **5a**$^-$ to give the dianion **5a**$^{2-}$. Cathodic potential: −1.1 to −1.3 V; recorded in THF.

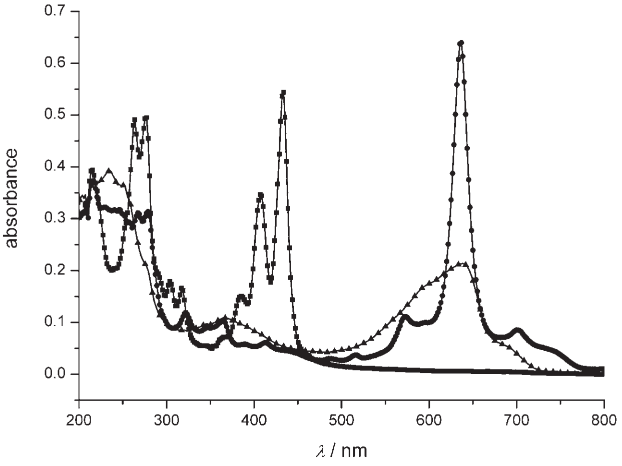

Figure 11. Comparison of the UV-visible absorption spectra of **5a** (■), **5a**$^-$ (●), and **5a**$^{2-}$ (▲).

Conclusions

The facile accessibility of DPDI by way of the thallium(I)-induced coupling of 1,8-diaminonaphthalene has provided a method of entry into the chemistry of 1,3,8,10-tetraazaperopyrene and its 2,9-disubstituted derivatives. The incorporation of four nitrogen atoms into their polycondensed aromatic core allows the modulation of their photophysics by way of protonation in condensed media and makes them reversible two-electron acceptors.

This first study of their synthesis and photo- and electrochemical behaviour has established that 1,3,8,10-tetraazaperopyrenes are promising candidates for further functionalisation and incorporation into complex functional aggregates. Moreover, the calculated electron affinity of parent compound **1** of −2 eV and the possibility of increasing this further by the introduction of electron-withdrawing substituents makes these materials promising candidates for the development of organic n-channel semiconductors.[4f,6] Such work is currently under way in our laboratory.

Experimental Section

All manipulations were performed under dried argon in standard (Schlenk) glassware which was flame dried with a Bunsen burner prior to use. Solvents were dried according to standard procedures and saturated with argon. The deuterated solvents used for the NMR spectroscopic measurements were degassed successively by three "freeze–pump–thaw" cycles and dried over 4 Å molecular sieves. Solids were separated from suspensions by centrifugation, thus avoiding filtration procedures. The centrifuge employed was a Rotina 48 (Hettich Zentrifugen, Tuttlingen, Germany) which was equipped with a specially designed Schlenk tube rotor.[33]

The ^{1}H and ^{13}C NMR spectra were recorded by using Bruker AVANCE 200, 400 and 600^{II+} spectrometers equipped with variable-temperature units. DTA and TGA measurements were carried out with a Mettler Toledo instrument equipped with a TG50 thermobalance and a TC15 TA controller. Elemental analyses were carried out in the Microanalytical Laboratory of the Chemistry Department at the University of Heidelberg. 4,9-Diamino-3,10-perylenequinone diimine (DPDI) was synthesised as reported previously.[18b] All other starting materials were obtained commercially and used without further purification.

Preparation of 1,3,8,10-tetraazaperopyrene (1): A suspension of DPDI (500 mg,1.6 mmol) in triethyl orthoformate (50 mL) and catalytic amounts of formic acid (1 mL) was refluxed for 48 h. After cooling to ambient temperature the precipitate was collected by filtration, washed with water, ethanol, acetone and pentane and dried in vacuo to yield 449 mg (1.4 mmol, 88 %). For further purification the brown solid was sublimed at 10^{-6} mbar and 250 °C. Dec >430 °C; ^{1}H NMR (600 MHz, [D$_1$]TFA, 295 K): $\delta = 10.57$ (d, $^3J = 9.6$ Hz, 4H), 10.26 (s, 2H), 9.24 ppm (d, $^3J = 7.7$ Hz, 4H). ^{13}C NMR (150 MHz, [D$_1$]TFA, 295 K): $\delta = 150.8$ (s, C$_{\text{Aryl}}$), 147.8 (d, CH$_{\text{Aryl}}$), 138.8 (d, CH$_{\text{Aryl}}$), 130.1 (s, C$_{\text{Aryl}}$), 126.0 (d, CH$_{\text{Aryl}}$), 120.4 (s, C$_{\text{Aryl}}$), 115.5 ppm (s, C$_{\text{Aryl}}$); HRMS (EI): *m/z* calcd for $C_{22}H_{10}N_4$: 330.0905; found: 330.0911; elemental analysis calcd (%) for $C_{22}H_{10}N_4$: C 79.99, H 3.05, N 16.96; found: C 80.15, H 3.26, N 16.75.

Preparation of 2,9-dimethyl-1,3,8,10-tetraazaperopyrene (2): Acetic anhydride (30 mL) was added to a suspension of DPDI (700 mg, 2.3 mmol) in nitrobenzene (50 mL) and the mixture was refluxed for 6 h. The mixture was allowed to cool to room temperature overnight. The resulting suspension was filtered, washed several times with nitrobenzene and finally with ethanol (200 mL). The brown solids were recrystallised from nitrobenzene to give a brown yellowish powder (550 mg, 1.5 mmol, 65 %). Dec >400 °C; ^{1}H NMR (600 MHz, [D$_1$]TFA, 295 K): $\delta = 10.59$ (d, $^3J = 9.6$ Hz, 4H), 9.17 (d, $^3J = 9.4$ Hz, 4H), 2.22 ppm (s, 6H); ^{13}C NMR (150 MHz, [D$_1$]TFA, 295 K): $\delta = 160.8$ (s, C$_{\text{Aryl}}$), 151.2 (s, C$_{\text{Aryl}}$), 138.5 (d, CH$_{\text{Aryl}}$), 129.7 (s, C$_{\text{Aryl}}$), 125.6 (d, CH$_{\text{Aryl}}$), 120.5 (s, C$_{\text{Aryl}}$), 114.0 (s, C$_{\text{Aryl}}$), 18.6 ppm (q, CH$_3$); HRMS (EI): *m/z* calcd for $C_{24}H_{14}N_4$: 358.1218; found: 358.1240; elemental analysis calcd (%) for $C_{24}H_{14}N_4$: C 80.43, H 3.94, N 15.63; found: C 80.35, H 4.14, N 15.40.

Preparation of 2,9-di-*tert*-butyl-1,3,8,10-tetraazaperopyrene (3): Trimethylacetyl chloride (241 mg, 2 mmol) and triethylamine (0.4 mL, 2.8 mmol) were added to a suspension of DPDI (310 mg, 1 mmol) in THF (30 mL). The mixture was heated at 70 °C for 72 h. The solvent was removed under reduced pressure, the remaining residue was washed three times with water (3×30 mL), acetone and pentane and the orange solid was dried in vacuo, to give the desired product (282 mg, 0.6 mmol, 64 %). Dec. >420 °C; ^{1}H NMR (600 MHz, [D$_1$]TFA, 295 K): $\delta = 10.42$ (d, $^3J = 9.6$ Hz, 4H), 9.18 (d, $^3J = 9.4$ Hz, 4H), 1.94 ppm (s, 18H); ^{13}C NMR (150 MHz, [D$_1$]TFA, 295 K): $\delta = 169.8$ (s, C$_{\text{Aryl}}$), 151.6 (s, C$_{\text{Aryl}}$), 137.4 (d, CH$_{\text{Aryl}}$), 129.4 (s, C$_{\text{Aryl}}$), 126.5 (d, CH$_{\text{Aryl}}$), 120.6 (s, C$_{\text{Aryl}}$), 113.3 (s, C$_{\text{Aryl}}$), 39.9 (s, C(CH$_3$)$_3$), 27.6 ppm (q, C(CH$_3$)$_3$); HRMS (FAB): *m/z* calcd for $C_{30}H_{27}N_4$: 443.2236; found: 443.2192; elemental analysis calcd (%) for $C_{30}H_{26}N_4$: C 81.42, H 5.92, N 12.66; found: C 81.53, H 5.81, N 12.66.

Preparation of 2,9-diadamantyl-1,3,8,10-tetraazaperopyrene (4): 1-Adamantanecarboxylic acid chloride (2.0 g, 10.1 mmol) was added to a suspension of DPDI (330 mg, 1.1 mmol) in nitrobenzene (50 mL) and the mixture was refluxed for 6 h. The mixture was allowed to cool to room temperature overnight. The resulting suspension was filtered, washed several times with nitrobenzene and finally with ethanol (200 mL). The brown solids were recrystallised from nitrobenzene to give an orange powder (448 mg, 0.7 mmol, 68 %). Dec >440 °C; ^{1}H NMR (600 MHz, [D$_1$]TFA, 295 K): $\delta=10.35$ (d, $^{3}J=9.6$ Hz, 4 H), 9.13 (d, $^{3}J=9.4$ Hz, 4 H), 2.53 (m, 12 H), 2.35 (m, 6 H), 2.00 ppm (m, 12 H); ^{13}C NMR (150 MHz, [D$_1$]TFA, 295 K): $\delta=171.5$ (s, C$_{\text{Aryl}}$), 153.7 (s, C$_{\text{Aryl}}$), 139.4 (d, CH$_{\text{Aryl}}$), 131.4 (s, C$_{\text{Aryl}}$), 128.6 (d, CH$_{\text{Aryl}}$), 122.5 (s, C$_{\text{Aryl}}$), 115.7 (s, C$_{\text{Aryl}}$), 44.7 (q, C$_{\text{Ad}}$), 42.1 (t, CH$_2$), 37.4 (d, CH), 30.1 ppm (t, CH$_2$); HRMS (EI): *m*/*z* calcd for $C_{42}H_{38}N_4$: 598.3096; found: 598.3064; elemental analysis calcd (%) for $C_{42}H_{38}N_4$: C 84.25, H 6.40, N 9.36; found: C 84.51, H 6.39, N 9.33.

Preparation of 2,9-Bis(undecyl)-1,3,8,10-tetraazaperopyrene (5 a): Lauroyl chloride (438 mg, 2 mmol) and triethylamine (0.4 mL, 2.8 mmol) were added to a suspension of DPDI (310 mg, 1 mmol) in THF (30 mL). The mixture was heated at 70 °C for 72 h. The solvent was removed under reduced pressure before the remaining residue was washed with water (3× 30 mL), acetone and pentane and the brown solid was dried in vacuo to give the title compound (435 mg, 0.7 mmol, 70 %). Dec >435 °C; ^{1}H NMR (400 MHz, CDCl$_3$, 295 K): $\delta=9.38$ (d, $^{3}J=9.6$ Hz, 4 H), 8.45 (d, $^{3}J=9.4$ Hz, 4 H), 3.48 (t, 4 H), 2.17 (quint, 4 H), 1.62 (quint, 4 H), 1.49 (quint, 4 H), 1.30 (m, 24 H), 0.91 ppm (t, 6 H); ^{13}C NMR (100 MHz, CDCl$_3$, 295 K): $\delta=169.6$ (s, C$_{\text{Aryl}}$), 153.4 (s, C$_{\text{Aryl}}$), 130.0 (d, CH$_{\text{Aryl}}$), 129.1 (d, CH$_{\text{Aryl}}$), 125. 5 (s, C$_{\text{Aryl}}$), 120.5 (s, C$_{\text{Aryl}}$), 114.2 (s, C$_{\text{Aryl}}$), 40.9, 32.0, 30.0, 30.0, 29.7, 29.7, 29.6, 29.6, 29.4, 22.7 (t, CH$_2$), 14.2 ppm (q, CH$_3$); HRMS (FAB): *m*/*z* calcd for $C_{44}H_{55}N_4$: 639.4427; found: 639.4418; elemental analysis calcd (%) for $C_{44}H_{54}N_4{\cdot}H_2O$: C 80.44, H 8.59, N 8.53; found: C 80.30, H 8.74, N 8.31.

Preparation of 2,9-bis(pentadecyl)-1,3,8,10-tetraazaperopyrene (5 b): Palmitoyl chloride (853 mg, 3.1 mmol) and triethylamine (0.6 mL, 4.5 mmol) were added to a suspension of DPDI (480 mg, 1.5 mmol) in THF (30 mL) . The mixture was heated at 70 °C for 72 h. The solvent was removed under reduced pressure before the remaining residue was washed with water (3×30 mL), acetone and pentane and the orange solid was dried in vacuo to give the title compound (786 mg, 1.0 mmol, 67 %). Dec >430 °C; ^{1}H NMR (400 MHz, CDCl$_3$, 323 K): $\delta=9.51$ (d, $^{3}J=9.5$ Hz, 4 H), 8.55 (d, $^{3}J=9.4$ Hz, 4 H), 3.52 (t, 4 H), 2.21 (quint, 4 H), 1.64 (quint, 4 H), 1.51 (quint, 4 H), 1.30 (m, 40 H), 0.92 ppm (t, 6 H); ^{13}C NMR (100 MHz, CDCl$_3$, 323 K): $\delta=169.7$ (s, C$_{\text{Aryl}}$), 153.7 (s, C$_{\text{Aryl}}$), 130.4 (d, CH$_{\text{Aryl}}$), 129.3 (d, CH$_{\text{Aryl}}$), 125.9 (s, C$_{\text{Aryl}}$), 120.9 (s, C$_{\text{Aryl}}$), 114.5 (s, C$_{\text{Aryl}}$), 40.9, 32.0, 30.0, 29.9, 29.7, 29.7, 29.7, 29.6, 29.6, 29.5, 29.5, 29.4, 29.4, 22.7 (t, CH$_2$), 14.2 ppm (q, CH$_3$); HRMS (FAB): *m*/*z* calcd for $C_{52}H_{71}N_4$: 751.5679; found: 751.5658; elemental analysis calcd (%) for $C_{52}H_{79}N_4{\cdot}C_4H_8O_1$: C 81.70, H 9.55, N 6.81; found: C 81.52, H 9.60, N 7.09.

Preparation of 2,9-bis(2-bromophenyl)-1,3,8,10-tetraazaperopyrene (6): 2-Bromobenzoyl chloride (4.0 g, 18.2 mmol) was added to a suspension of DPDI (600 mg, 1.9 mmol) in nitrobenzene (50 mL) and the mixture was heated at reflux for 6 h. The mixture was allowed to cool to room temperature overnight. The resulting suspension was filtered, washed several times with nitrobenzene and finally with ethanol (200 mL). The brown solids were recrystallised from nitrobenzene to give an orange powder (684 mg, 1.1 mmol, 58 %). Dec >415 °C; ^{1}H NMR (600 MHz, [D$_1$]TFA, 295 K): $\delta=10.54$ (d, $^{3}J=9.6$ Hz, 4 H), 9.25 (d, $^{3}J=9.3$ Hz, 4 H), 8.03 (d, $^{3}J=7.4$ Hz, 2 H) 7.92 (d, $^{3}J=8.1$ Hz, 2 H), 7.69 (t, 2 H), 7.65 ppm (t, 2 H); ^{13}C NMR (150 MHz, [D$_1$]TFA, 295 K): $\delta=157.5$ (s, C$_{\text{Aryl}}$), 151.3 (s, C$_{\text{Aryl}}$), 138.5 (d, CH$_{\text{Aryl}}$), 134.6 (d, CH$_{\text{Aryl}}$), 134.3 (d, CH$_{\text{Aryl}}$), 132.3 (d, CH$_{\text{Aryl}}$), 131.3 (s, C$_{\text{Aryl}}$), 130.0 (s, C$_{\text{Aryl}}$), 128.4 (d, CH$_{\text{Aryl}}$), 126.2 (d, CH$_{\text{Aryl}}$), 121.2 (s, C$_{\text{Aryl}}$), 120.5 (s, C$_{\text{Aryl}}$), 114.0 ppm (s, C$_{\text{Aryl}}$); HRMS (EI): *m*/*z* calcd for $C_{34}H_{16}N_4Br_2$: 639.9721; found: 639.9720; elemental analysis calcd (%) for $C_{34}H_{16}N_4Br_2$: C 63.77, H 2.52, N 8.75; found: C 63.56, H 2.61, N 8.60.

Preparation of 2,9-bis(2-carboxyphenyl)-1,3,8,10-tetraazaperopyrene (7): Phthalic anhydride (2.0 g, 13.5 mmol) was added to a suspension of DPDI (400 mg, 1.3 mmol) in nitrobenzene (50 mL) and the mixture was refluxed for 6 h. The mixture was allowed to cool to room temperature overnight. The resulting suspension was filtered, washed several times with nitrobenzene and finally with ethanol (200 mL). The brown solid was extracted by boiling in a 2 M aqueous potassium hydroxide solution (250 mL), filtered when hot and after cooling to ambient temperature the solution was acidified by addition of concentrated hydrochloric acid. The red-brown precipitate was collected by centrifugation, washed several times with water, ethanol, acetone and finally dried in vacuo to give a shiny black solid yield (296 mg, 0.6 mmol, 46 %). Dec >340 °C; ^{1}H NMR (600 MHz, [D$_1$]TFA, 295 K): $\delta=10.55$ (d, $^{3}J=9.6$ Hz, 4 H), 9.24 (d, $^{3}J=9.3$ Hz, 4 H), 8.53 (d, $^{3}J=7.6$ Hz, 2 H), 8.01 ppm (m, 6 H); ^{13}C NMR (150 MHz, [D$_1$]TFA, 295 K): $\delta=170.8$ (s, COOH), 159.2 (s, C$_{\text{Aryl}}$), 151.0 (s, C$_{\text{Aryl}}$), 138.5 (d, CH$_{\text{Aryl}}$), 134.5 (d, CH$_{\text{Aryl}}$), 133.2 (d, CH$_{\text{Aryl}}$), 132.5 (d, CH$_{\text{Aryl}}$), 132.0 (s, C$_{\text{Aryl}}$), 131.2 (d, CH$_{\text{Aryl}}$), 130.0 (s, C$_{\text{Aryl}}$), 128.0 (s, C$_{\text{Aryl}}$), 126.1 (d, CH$_{\text{Aryl}}$), 120.6 (s, C$_{\text{Aryl}}$), 114.2 ppm (s, C$_{\text{Aryl}}$); elemental analysis calcd (%) for $C_{36}H_{18}N_4O_4{\cdot}H_2O$: C 73.46, H 3.43, N 9.52; found: C 73.80, H 3.59, N 9.64.

Conversion of 2,9-bis(2-bromophenyl)-1,3,8,10-tetraazaperopyrene (6) to 2,9-bis(2-carboxyphenyl)-1,3,8,10-tetraazaperopyrene (7): *n*BuLi (2.5 M in hexane, 0.2 mL, 0.5 mmol) was added to a suspension of compound **8** (100 mg, 0.16 mmol) in THF at −30 °C and stirred for 30 min. The mixture was treated with an excess of freshly crushed carbon dioxide. The volatiles were removed in vacuo and the residue was extracted with a 2 M aqueous solution of sodium hydroxide. The aqueous solution was filtered and the filtrate was neutralised to pH 7 by using hydrochloric acid. The precipitate was collected by filtration, washed with water, ethanol, acetone and pentane and dried in vacuo. The sample of compound **7** prepared by this route had the same analytical and spectroscopic properties as that prepared by the method described in the previous section (89 mg, 0.15 mmol, 94 %).

Computational details: The five structures **1**, **1**H^{+}, **1**H$_2$$^{2+}$, **1**H$_3$$^{3+}$ and **1**H$_4$$^{4+}$ were calculated by using the Gaussian 03 program.[34] The structures were optimised without symmetry constraints at the DFT/B3PW91 level of theory by using the 6-31g(d,p) basis set. Each geometry optimisation was followed by a frequency calculation to ensure the absence of any imaginary frequencies and thus ensuring that the calculated structure was a minimum on the potential energy surface. The thermodynamic data used to calculate the PA were obtained from a frequency calculation. The CPCM system was used to model the PA in solution and with the B3PW91/6-31g(d,p)-optimised structures a frequency calculation was performed at the B3LYP/3-21g level of theory. The transition energies for the protonation of **1** to **1**H^{+}, **1**H$_2$$^{2+}$, **1**H$_3$$^{3+}$ and **1**H$_4$$^{4+}$ in the gas phase were obtained by TDDFT based on the B3PW91 functional by using the 6-31g(d,p) basis set, as implemented in the Gaussian 03 program package.[34] To investigate the influence of solvation on the transition energies a TDDFT calculation combined with a CPCM calculation was performed. Toluene was used as the solvent, as defined in the Gaussian 03 program. [34] For concentrated sulfuric acid a dielectric constant of 100, a radius of 2.25 Å and a density of 0.0062 Å^{-3} were used. For trifluoroacetic acid the dielectric constant was set to 42, the radius to 3.12 Å and the density to 0.0081 Å^{-3}.

Crystal structure analysis of 6: Suitable single crystals of compound **6** were obtained by slow cooling of a solution in nitrobenzene. Intensity data were collected at a low temperature on a Bruker AXS Smart 1000 CCD diffractometer (Mo$_{K\alpha}$ radiation, graphite monochromator, $\lambda=0.71073$ Å). Data were corrected for Lorentz, polarisation and absorption effects (semiempirical, SADABS).[35] The structure was solved by direct methods and refined by full-matrix least-squares based on F^2 with all measured reflections. All non-hydrogen atoms were given anisotropic displacement parameters. Hydrogen atoms were input at calculated positions and refined with a riding model (Table 8).

The calculations were performed by using the programs SHELXS-86[36] and SHELXL-97[37] software packages. CCDC-632307 contains the supplementary crystallographic data for this paper. These data can be obtained free of charge from The Cambridge Crystallographic Data Centre via www.ccdc.cam.ac.uk/data_request/cif.

Spectroelectrochemistry: Spectroelectrochemical measurements were performed with an optically transparent, thin-layer, electrochemical

Table 8. Crystallographic data, structure solution and refinement for compound **6**.

	6
formula	$C_{34}H_{16}Br_2N_4$
M_r	640.33
T [K]	100(2)
crystal system	monoclinic
space group	$P2_1/c$
unit cell dimensions:	
a [Å]	4.0072(12)
b [Å]	11.814(4)
c [Å]	25.100(7)
γ [°]	92.891(7)
V [Å^3]	1186.7(6)
Z	2
ρ_{calcd} [Mg m^{-3}]	1.792
μ [mm^{-1}]	3.451
F_{000}	636
crystal size [mm^3]	0.20 × 0.10 × 0.10
θ range for data collection [°]	1.62–30.87
index ranges	$-5 \leq h \leq 5$
	$-16 \leq k \leq 0$
	$-35 \leq l \leq 4$
reflections collected	28053
independent reflections	3484 ($R_{int} = 0.0668$)
completeness to $\theta = 30.00°$ [%]	98.2
data/restraints/parameters	3484/0/181
goodness-of-fit on F^2	1.066
final R indices [$I > 2\sigma I$]	$R_1 = 0.0377$, $wR_2 = 0.0962$
R indices (all data)	$R_1 = 0.0541$, $wR_2 = 0.1028$
r.m.s. residual density	0.122
largest diff. peak and hole [e Å^{-3}]	0.902 and −0.507

cell;[38] the potential was controlled by a Voltalab 40 system from Radiometer Analytical which consisted of a PGZ301 potentiostat and Voltamaster 4 software; the spectra were recorded on a Carey 100 scan spectrometer from Varian. The electrolyte, ([NBu$_4$][PF$_6$], electrochemical grade) had been previously dried at 130 °C and was stored in a dessicator between measurements. A typical measurement was performed as follows: A Schlenk flask was dried in an oven at 130 °C prior to use and cooled to room temperature under a stream of dry nitrogen. The electrolyte and the compound to be measured were weighed into the flask, which was then evacuated and heated briefly to remove oxygen and moisture that had been introduced. The flask was then filled with dry N_2, re-evacuated and filled again with nitrogen twice and THF (freshly distilled from Na/K/benzophenone) was added through a syringe. The resulting solution was sonicated briefly to dissolve the solids and then degassed for ten minutes with a gentle stream of N_2 and the solution finally transferred to the OTTLE cell by syringe. A single scan (5 mV s^{-1}) was performed to locate the appropriate waves and determine reversibility at this low scan rate; a second scan was run for which UV/Vis spectra were recorded at different points during the reductions and again during the subsequent oxidations. In all cases the re-oxidation gave the original UV/Vis spectrum virtually unchanged.

Photophysical measurements: The UV-visible absorption spectra were recorded by using a Cary 5000 UV-visible/near-infrared spectrophotometer and were baseline- and solvent-corrected. Steady-state and time-resolved luminescence experiments were performed by using a HORIBA Jobin-Yvon IBH FL-322 Fluorolog 3 spectrometer equipped with a 450 W xenon arc lamp, double-grating excitation and emission monochromators (2.1 nm mm^{-1} dispersion, 1200 grooves mm^{-1}) and a Hamamatsu R928 photomultiplier tube or a TBX-4-X single-photon-counting detector. Emission and excitation spectra were corrected for source intensity (lamp and grating) and emission spectral response (detector and grating) by standard correction curves. Time-resolved measurements were performed by using the time-correlated single-photon-counting (TCSPC) option on the Fluorolog 3 instrument. NanoLEDs (295 or 402 nm, FWHM < 750 ps) with repetition rates between 10 kHz and 1 MHz were used to excite the sample. The excitation sources were mounted directly onto the sample chamber at 90° to a double-grating emission monochromator (2.1 nm mm^{-1} dispersion, 1200 grooves mm^{-1}) and collected with a TBX-4-X single-photon-counting detector. The photons collected at the detector were correlated by a time-to-amplitude converter (TAC) to the excitation pulse. Signals were collected by using an IBH DataStation Hub photon-counting module and data analysis was performed by using the commercially available DAS6 software (HORIBA Jobin Yvon IBH). The goodness-of-fit was assessed by minimising the reduced χ^2 function and by visual inspection of the weighted residuals. Luminescence quantum yields (Φ_{em}) were measured in optically dilute solutions (OD < 0.1 at excitation wavelength) and compared with reference emitters by using Equation (1),[39], in which A is the absorbance at the excitation wavelength (λ), I is the intensity of the excitation light at the excitation wavelength (λ), n is the refractive index of the solvent, D is the integrated intensity of the luminescence and Φ is the quantum yield. The subscripts r and x refer to the reference and the sample, respectively. All quantum yields were determined at identical excitation wavelengths for the sample and the reference, cancelling the $I(\lambda_r)/I(\lambda_x)$ term in the equation.

$$\Phi_x = \Phi_r \left[\frac{A_r(\lambda_r)}{A_x(\lambda_x)}\right] \left[\frac{I_r(\lambda_r)}{I_x(\lambda_x)}\right] \left[\frac{n_x^2}{n_r^2}\right] \left[\frac{D_x}{D_r}\right] \quad (1)$$

Two different quantum yield reference compounds were used: a degassed solution of perylene in ethanol ($\Phi = 0.92$) for the samples dissolved in toluene and an aqueous solution (0.1 M NaOH) of fluorescein ($\Phi = 0.87$) for measuring the quantum yields of the samples dissolved in acidic media. Perylene deaerated solutions were prepared by the freeze–pump–thaw technique.

Acknowledgements

We thank the Universities of Heidelberg and Münster and the Fonds der Chemischen Industrie for support of this work.

---

[1] a) R. G. Harvey, *Polycyclic Aromatic Hydrocarbons*, Wiley-VCH, New York, **1997**; b) *Topics in Current Chemistry, Vol. 196: Carbon Rich Compounds I* (Ed.: A. de Meijere), Springer, Berlin, **1998**; c) *Topics in Current Chemistry, Vol. 201: Carbon Rich Compounds II: Macrocyclic Oligoacetylenes and Other Linearly Conjugated Systems* (Ed.: A. de Meijere), Springer, Berlin, **1999**, *Vol. 201.*

[2] a) *Handbook of Conducting Polymers*, 2nd ed. (Eds.: T. A. Skotheim, R. L. Elsenbaumer, J. R. Reynolds), Marcel Dekker, New York, **1998**; b) *Semiconducting Polymers: Chemistry, Physics, and Engineering* (Eds.: G. Hadziioannou, P. F. van Hutten), Wiley-VCH, Weinheim, **2000**; c) *Electronic Materials: The Oligomer Approach* (Eds.: K. Müllen, G. Wegner) Wiley-VCH, Weinheim, **1998**.

[3] For the 2000 Nobel Prize lectures, see: a) H. Shirakawa, *Angew. Chem.* **2001**, *113*, 2642; *Angew. Chem. Int. Ed.* **2001**, *40*, 2574; b) A. G. MacDiarmid, *Angew. Chem.* **2001**, *113*, 2649; *Angew. Chem. Int. Ed.* **2001**, *40*, 2581; c) A. J. Heeger, *Angew. Chem.* **2001**, *113*, 2660; *Angew. Chem. Int. Ed.* **2001**, *40*, 2591.

[4] For recent reviews on organic electronics, see: a) U. Mitschke, P. Bäuerle, *J. Mater. Chem.* **2000**, *10*, 1471; b) F. Würthner, *Angew. Chem.* **2001**, *113*, 1069; *Angew. Chem. Int. Ed.* **2001**, *40*, 1037; c) H. E. Katz, Z. Bao, S. L. Gilat, *Acc. Chem. Res.* **2001**, *34*, 359; d) C. D. Dimitrakopoulos, P. R. Malenfant, *Adv. Mater.* **2002**, *14*, 99; e) M. Bendikov, F. Wudl, D. F. Perepichka, *Chem. Rev.* **2004**, *104*, 4891; f) C. R. Newman, C. D. Frisbie, F. D. A. da Silva, J.-L. Bredas, P. C. Ewbank, K. R. Mann, *Chem. Mater.* **2004**, *16*, 4436; g) J.-L. Bredas, D. Beljonne, V. Coropceanu, J. Cornil, *Chem. Rev.* **2004**, *104*, 4971; h) F. Würthner, R. Schmidt, *Chem. Phys.* **2006**, *7*, 793; i) J. E. Anthony, *Chem. Rev.* **2006**, *106*, 5028.

[5] For studies on *N*-heterocyclic PAHs, see: a) C. J. Tonzola, M. M. Alam, W. Kaminsky, S. A. Jenekhe, *J. Am. Chem. Soc.* **2003**, *125*,

13548; b) J.-I. Nishida, Naraso, S. Murai, E. Fujiwara, H. Tada, M. Tomura, Y. Yamashita, *Org. Lett.* **2004**, *6*, 2007; c) O. Schmelz, A. Mews, T. Basché, A. Herrmann, K. Müllen, *Langmuir* **2001**, *17*, 2861.

[6] For a detailed computational study on the n-type semiconducting properties of nitrogen-rich oligoacenes, see: M. Winkler, K. N. Houk, *J. Am. Chem. Soc.* **2007**, *129*, 1805.

[7] For studies of heterocyclic PAHs in connection with organic semiconductivity, see: a) M. Tadokoro, S. Yasuzuka, M. Nakamura, T. Shinoda, T. Tatenuma, M. Mitsumi, Y. Qzawa, K. Toriumi, H. Yoshino, D. Shiomi, K. Sato, T. Takui, T. Mori, K. Murata, *Angew. Chem.* **2006**, *118*, 5268; *Angew. Chem. Int. Ed.* **2006**, *45*, 5144; b) K. A. Hutchison, G. Srdanov, R. Hicks, H. Yu, F. Wudl, T. Strassner, M. Nendel, K. N. Houk, *J. Am. Chem. Soc.* **1998**, *120*, 2989; c) F. Wudl, P. A. Koutentis, A. Weiz, B. Ma, T. Strassner, K. N. Houk, S. I. Khan, *Pure Appl. Chem.* **1999**, *71*, 295; d) A. E. Riley, G. W. Mitchell, P. A. Koutentis, M. Bendikov, P. Kaszynki, F. Wudl, S. H. Tolbert, *Adv. Funct. Mater.* **2003**, *13*, 531; e) C. P. Constaninides, P. A. Koutentis, J. Schatz, *J. Am. Chem. Soc.* **2004**, *126*, 16232; f) P. Langer, A. Bodtke, N. N. R. Saleh, H. Görls, P. R. Schreiner, *Angew. Chem.* **2005**, *117*, 5389; *Angew. Chem. Int. Ed.* **2005**, *44*, 5255; g) Q. Miao, T. Q. Nguyen, T. Someya, G. B. Blanchet, C. Nuckolls, *J. Am. Chem. Soc.* **2003**, *125*, 10284; h) Y. Ma, Y. Sun, Y. Liu, J. Gao, S. Chen, X. Sun, W. Qiu, G. Yu, G. Cui, W. Hu, D. Zhu, *J. Mater. Chem.* **2005**, *15*, 4894.

[8] a) J.-M. Lehn, *Supramolecular Chemistry*, VCH, Weinheim, **1995**; b) *Comprehensive Supramolecular Chemistry, Vol. 1–11* (Eds.: J.-M. Lehn, J. L. Atwood, J. E. D. Davies, D. D. MacNicol, F. Vögtle), Pergamon, Oxford, **1996**.

[9] a) H. L. Anderson, C. A. Hunter, M. Nafees Meah, J. K. M. Sanders, *J. Am. Chem. Soc.* **1990**, *112*, 5780; b) M. Fujita, *J. Synth. Org. Chem. Jpn.* **1996**, *54*, 953; c) P. J. Stang, *Chem. Eur. J.* **1998**, *4*, 19; d) R. H. Vreekamp, W. Verboom, D. Reinhoudt, *J. Org. Chem.* **1996**, *61*, 4282; e) S. Subramanian, M. J. Zaworotko, *Angew. Chem.* **1995**, *107*, 2295; *Angew. Chem. Int. Ed. Engl.* **1995**, *34*, 2127 (2561); f) S. Valiyaveettil, V. Enkelmann, G. Moeßner, K. Müllen, *Macromol. Symp.* **1996**, *102*, 165; g) D. Gut, A. Rudi, J. Kopilov, I. Goldberg, M. Kol, *J. Am. Chem. Soc.* **2002**, *124*, 5449; h) E. C. Glazer, Y. Tor, *Angew. Chem.* **2002**, *114*, 4194; *Angew. Chem. Int. Ed.* **2002**, *41*, 4022; i) D. Gut, I. Goldberg, M. Kol, *Inorg. Chem.* **2003**, *42*, 3483; j) O. M. Yaghi, H. Li, C. Davis, D. Richardson, T. L. Groy, *Acc. Chem. Res.* **1998**, *31*, 474; k) O. M. Yaghi, G. M. Li, *Angew. Chem.* **1995**, *107*, 232; *Angew. Chem. Int. Ed. Engl.* **1995**, *34*, 207; l) O. M. Yaghi, H. L. Li, T. L. Groy, *Inorg. Chem.* **1997**, *36*, 4292.

[10] a) Y. Avlasevich, K. Müllen, *Chem. Commun.* **2006**, *42*, 4440; b) A. Herrmann, K. Müllen, *Chem. Lett.* **2006**, *9*, 978; c) M. Cotlet, T. Vosch, S. Habuchi, T. Weil, K. Müllen, J. Hofkens, F. De Schryver, *J. Am. Chem. Soc.* **2005**, *127*, 9760; d) T. Weil, M. Abdalla, C. Jatzke, J. Hengstler, K. Müllen, *Biomacromolecules* **2005**, *6*, 68; e) A. Margineanu, J. Hofkens, M. Cotlet, S. Habuchi, A. Stefan, J. Qu, C. Kohl, K. Müllen, J. Vercammen, Y. Engelborghs, T. Gensch, F. C. De Schryver, *J. Phys. Chem. B* **2004**, *108*, 12242.

[11] E. Clar, *Ber. Dtsch. Chem. Ges.* **1943**, *76*, 458.

[12] a) U. Wenzel, H.-G. Löhmannsröben, *J. Photochem. Photobiol., A,* **1996**, 13; b) R. Boschi, E. Clar, W. Schmidt, *J. Chem. Phys.* **1974**, *60*, 4406; c) M. Zander, U. Breymann, H. Dreeskamp, E. Koch, *Z. Naturforsch., A* **1977**, *32*, 1561; d) I. Bergmann, *Trans. Faraday Soc.* **1954**, *50*, 829; e) H. Dreeskamp, E. Koch, M. Zander, *Z. Naturforsch., A* **1975**, *30*, 1311; f) U. Breymann, H. Dreeskamp, E. Koch, M. Zander, *Chem. Phys. Lett.* **1978**, *59*, 68; g) Y. Kamura, H. Inokuchi, J. Aoki, D. Fujisawa, *Chem. Phys. Lett.* **1977**, *46*, 356; h) Y. Mishashita, T. Okuyama, K. Yamaura, K. Jinno, S. I. Sasaki, *Anal. Chim. Acta* **1987**, *202*, 237; i) I. Agranat, M. R. Suissa, *Polycycl. Aromat. Compd.* **1992**, *3*, 51.

[13] M. Kardos, Ger. Pat.276357, **1913**.

[14] A. Slama-Schwok, J. Jazwinski, A. Béré, T. Montenay-Garestier, M. Rougée, C. Hélène, J.-M. Lehn, *Biochem.* **1989**, *28*, 3227.

[15] P. J. Stang, D. H. Cao, S. Saito, A. M. Arif, *J. Am. Chem. Soc.* **1995**, *117*, 6273.

[16] This particular limitation has recently been overcome by Würthner and co-workers by way of introducing substituents in the bay positions of the central perylenic core and thus permitting a systematic study of their supramolecular complexes with Pd^{II} and Pt^{II} in solution: a) F. Würthner, A. Sautter, C. Thalacker, *Angew. Chem.*, **2000**, *112*, 1298; *Angew. Chem. Int. Ed.* **2000**, *39*, 1243; b) A. Sautter, D. G. Schmid, G. Jung, F. Würthner, *J. Am. Chem. Soc.* **2001**, *123*, 5424; c) A. Sautter, C. Thalacker, F. Würthner, *Angew. Chem.* **2001**, *113*, 4557; *Angew. Chem. Int. Ed.* **2001**, *40*, 4425; d) F. Würthner, A. Sautter, J. Schilling, *J. Org. Chem.* **2002**, *67*, 3037; e) F. Würthner, V. Stepanenko, A. Sautter, *Angew. Chem.* **2006**, *118*, 1973; *Angew. Chem. Int. Ed.* **2006**, *45*, 1939.

[17] A. Zinke, W. Hirsch, E. Brozek, *Monatsh. Chem.* **1929**, *51*, 205.

[18] a) K. W. Hellmann, C. H. Galka, I. Rüdenauer, L. H. Gade, I. J. Scowen, M. McPartlin, *Angew. Chem.* **1998**, *110*, 2053; *Angew. Chem. Int. Ed.* **1998**, *37*, 1948; b) L. H. Gade, C. H. Galka, K. W. Hellmann, R. M. Williams, L. De Cola, I. J. Scowen, M. McPartlin, *Chem. Eur. J.* **2002**, *8*, 3732; c) L. H. Gade, C. H. Galka, R. M. Williams, L. De Cola, M. McPartlin, L. Chi, B. Dong, *Angew. Chem.* **2003**, *115*, 2781; *Angew. Chem. Int. Ed.* **2003**, *42*, 2677; d) M. Stöhr, M. Wahl, C. H. Galka, T. Riehm, T. A. Jung, L. H. Gade, *Angew. Chem.* **2005**, *117*, 7560; *Angew. Chem. Int. Ed.* **2005**, *44*, 7394; e) M. Wahl, M. Stöhr, H. Spillmann, T. A. Jung, L. H. Gade, *Chem. Commun.* **2007**, 1349.

[19] a) F. Würthner, *Chem. Commun.* **2004**, 1564; b) G. Seybold, G. Wagenblast, *Dyes Pigm.* **1989**, *11*, 303; c) G. Seybold, A. Stange (BASF AG), Ger. Pat. DE 3545004, **1987**; [*Chem. Abstr.* **1988**, *108*, 77134c].

[20] a) K. Kozawa, T. Uchida, *Acta Crystallogr., Sect. A* **1983**, *39*, 1233; b) P. L. Wash, S. H. Ma, U. Obst, J. Rebek, Jr., *J. Am. Chem. Soc.* **1999**, *121*, 7973; c) H. Yamochi, G. Saito, T. Suyamo, M. Kinoshita, C. Katayama, J. Tanaka, *Chem. Lett.* **1986**, 1303; d) P. Osswald, D. Leusser, D. Stalke, F. Würthner, *Angew. Chem.* **2005**, *117*, 254; *Angew. Chem. Int. Ed.* **2005**, *44*, 250; e) Z. J. Chen, M. G. Debije, T. Debaerdemaeker, P. Osswald, F. Würthner, *ChemPhysChem* **2004**, *5*, 137; f) F. Würthner, V. Stepanenko, Z. J. Chen, C. R. Saha-Moller, N. Kocher, D. Stalke, *J. Org. Chem.* **2004**, *69*, 7933; g) J. Tanaka, *Bull. Chem. Soc. Jpn.* **1963**, *36*, 1237; h) K. A. Kerr, *Acta Crystallogr., Sect. A* **1966**, *21*, 119; i) L. Feiler, H. Langhals, K. Polborn, *Liebigs Ann.* **1995**, 1229; j) T. Ogawa, K. Kuwamoto, S. Isoda, T. Kobayashi, N. Karl, *Acta Crystallogr., Sect. B* **1999**, *55*, 123; k) H. Langhals, *Heterocycles* **1995**, *40*, 477.

[21] a) F. Graser, E. Hädicke, *Liebigs Ann. Chem.* **1980**, 1994; b) F. Graser, E. Hädicke, *Liebigs Ann. Chem.* **1984**, 483; c) E. Hädicke, F. Graser, *Acta Crystallogr., Sect. C* **1986**, *42*, 189; d) E. Hädicke, F. Graser, *Acta Crystallogr., Sect. C* **1986**, *42*, 195; e) G. Klebe, F. Graser, E. Hädicke, J. Berndt, *Acta Crystallogr., Sect. B* **1989**, *45*, 69; f) P. Zugmaier, J. Duff, T. L. Bluhm, *Cryst. Res. Technol.* **2000**, *35*, 1095.

[22] a) L. Feiler, H. Langhals, K. Polborn, *Liebigs Ann.* **1995**, 1229; b) H. Langhals, *Helv. Chim. Acta* **2005**, *88*, 1309; c) M. Sadrai, G. R. Bird, *Opt. Commun.* **1984**, *51*, 62–64; d) H. G. Löhmannsröben, H. Langhals, *Appl. Phys. B* **1989**, *48*, 449; e) W. E. Ford, P. V. Kamat, *J. Phys. Chem.* **1987**, *91*, 6373; f) U. Rohr, P. Schlichting, A. Böhm, M. Groß, K. Meerholz, C. Bräuchle, K. Müllen, *Angew. Chem.* **1998**, *110*, 1463; *Angew. Chem. Int. Ed.* **1998**, *37*, 1434; g) H. Langhals, J. Karolin, L. B. A. Johannson, *J. Chem. Soc., Faraday Trans.* **1998**, *94*, 2919.

[23] a) W. L. Jorgensen, J. M. Briggs, J. Gao, *J. Am. Chem. Soc.* **1987**, *109*, 6857; b) W. L. Jorgensen, J. M. Briggs, *J. Am. Chem. Soc.*, **1989**, *111*, 4190; c) C. Lim, D. Bashford, M. Karplus, *J. Phys. Chem.* **1991**, *95*, 5610; d) M. J. Potter, M. K. Gilson, J. A. McCammon, *J. Am. Chem. Soc.* **1994**, *116*, 10298; e) E. Rajasekaran, B. Jayaram, B. Honig, *J. Am. Chem. Soc.* **1994**, *116*, 8238; f) K. Daasbjerg, *Acta Chem. Scand.* **1995**, *49*, 878; g) M. Perakyla, *J. Org. Chem.* **1996**, *61*, 7420; h) F. Figueirido, G. S. Del Buono, R. M. Levy, *J. Phys. Chem.* **1996**, *100*, 6389; i) J. Li, C. L. Fisher, J. L. Chen, D. Bashford, L. Noodleman, *Inorg. Chem.* **1996**, *35*, 4694; j) M. J. Perakyla, *J. Am. Chem. Soc.* **1998**, *120*, 12895; k) G. Schüürmann, M. Cossi, V. Barone, J. Tomasi, *J. Phys. Chem. A* **1998**, *102*, 6706; l) C. O. Silva,

E. C. da Silva, M. A. C. Nascimento, *J. Phys. Chem. A* **2000**, *104*, 2402; m) D. M. Chipman, *J. Phys. Chem. A* **2002**, *106*, 7413.
[24] a) A. M. Toth, M. D. Liptak, D. L. Phillips, G. C. Shields, *J. Chem. Phys.* **2001**, *114*, 4595; b) M. D. Liptak, G. C. Shields, *J. Am. Chem. Soc.* **2001**, *123*, 7314.
[25] a) M. D. Tissandier, A. C. Kenneth, W. Y. Feng, E. Gundlach, M. H. Cohen, A. D. Earhart, J. V. Coe, *J. Phys. Chem. A* **1998**, *102*, 7787; b) D. M. Chipman, *J. Phys. Chem. A* **2002**, *106*, 7413.
[26] S. Hwang, Y. H. Jang, D. S. Chung, *Bull. Korean Chem. Soc.* **2005**, *26*, 585.
[27] A. M. Magill, K. J. Cavell, B. F. Yates, *J. Am. Chem. Soc.* **2004**, *126*, 8717.
[28] a) I. A. Topol, G. J. Tawa, S. K. Burt, A. A. Rashin, *J. Phys. Chem. A* **1997**, *101*, 10075; b) R. Scholz, A. Yu, D. R. T. Zahn, M. Schreiber, *Phys. Rev. B* **2005**, *72*, 245208-1.
[29] a) R. van Leeuwen, E. J. Baerends, *Phys. Rev. A* **1994**, *49*, 2421; b) M. E. Casida, C. Jamorski, K. C. Casida, D. R. Salahub, *J. Chem. Phys.* **1998**, *108*, 4439; c) R. E. Stratmann, G. E. Scuseria, M. J. Frisch, *J. Chem. Phys.* **1998**, *109*, 8218.
[30] J. N. Demas, G. A. Crosby *J. Phys. Chem.* **1971**, *75*, 991.
[31] W. R. Dawson, M. W. Windsor *J. Phys. Chem.* **1968**, *72*, 3251.
[32] M. D. Ward, *Chem. Soc. Rev.* **1995**, *24*, 121.
[33] K. W. Hellmann, L. H. Gade, *Verfahrenstechnik* **1997**, *5*, 70.
[34] Gaussian 03, Revision B.03, M. J. Frisch, G. W. Trucks, H. B. Schlegel, G. E. Scuseria, M. A. Robb, J. R. Cheeseman, J. A. Montgomery, Jr., T. Vreven, K. N. Kudin, J. C. Burant, J. M. Millam, S. S. Iyengar, J. Tomasi, V. Barone, B. Mennucci, M. Cossi, G. Scalmani, N. Rega, G. A. Petersson, H. Nakatsuji, M. Hada, M. Ehara, K. Toyota, R. Fukuda, J. Hasegawa, M. Ishida, T. Nakajima, Y. Honda, O. Kitao, H. Nakai, M. Klene, X. Li, J. E. Knox, H. P. Hratchian, J. B. Cross, V. Bakken, C. Adamo, J. Jaramillo, R. Gomperts, R. E. Stratmann, O. Yazyev, A. J. Austin, R. Cammi, C. Pomelli, J. W. Ochterski, P. Y. Ayala, K. Morokuma, G. A. Voth, P. Salvador, J. J. Dannenberg, V. G. Zakrzewski, S. Dapprich, A. D. Daniels, M. C. Strain, O. Farkas, D. K. Malick, A. D. Rabuck, K. Raghavachari, J. B. Foresman, J. V. Ortiz, Q. Cui, A. G. Baboul, S. Clifford, J. Cioslowski, B. B. Stefanov, G. Liu, A. Liashenko, P. Piskorz, I. Komaromi, R. L. Martin, D. J. Fox, T. Keith, M. A. Al-Laham, C. Y. Peng, A. Nanayakkara, M. Challacombe, P. M. W. Gill, B. Johnson, W. Chen, M. W. Wong, C. Gonzalez, J. A. Pople, Gaussian, Inc., Wallingford, CT, **2004**.
[35] SADABS-2004/1, G. M. Sheldrick, Bruker AXS, Madison, **2004**.
[36] SHELXS-86, G. M. Sheldrick, University of Göttingen, Göttingen (Germany), **1986**; G. M. Sheldrick, *Acta Crystallogr. Sect. A* **1990**, *46*, 467.
[37] SHELXL-97, G. M. Sheldrick, University of Göttingen, Göttingen (Germany), **1997**.
[38] a) M. Krejcik, M. Danek, F. Hartl, *J. Electroanal. Chem.* **1991**, *317*, 179; b) F. Hartl, H. Luyten, H. A. Nieuwenhuis, G. C. Schoemaker, *Appl. Spectrosc.* **1994**, *48*, 1522.
[39] D. F. Eaton, *Pure Appl. Chem.* **1988**, *60*, 1107.

Received: March 8, 2007